MARS SCIENCE LABORATORY ALPHA PARTICLE X-RAY SPECTROMETER ATMOSPHERIC RESULTS THROUGH EARLY MARS YEAR 35: A COMPARISON WITH OPPORTUNITY APXS, MSL SAM, AND MARS MODEL FOR PREDICTION ACROSS SCALES. S. J. VanBommel[1], Y. Lian[2], R. Gellert[3], J. A. Berger[4], N. I. Boyd[3], V. A. Flood[3], J. U. Hanania[3], M. McCraig[3], C. D. O'Connell-Cooper[5], M. I. Richardson[2], L. M. Thompson[5], B. J. Wilhelm[3], and M. G. Trainer[6], [1]McDonnell Center for the Space Sciences, Department of Earth and Planetary Sciences, Washington University in Saint Louis, [2]Aeolis Research, [3]University of Guelph, [4]NASA Johnson Space Center, [5]University of New Brunswick, [6]NASA Goddard.

Introduction: Alpha Particle X-ray Spectrometer (APXS) instruments have flown on each of the Mars Exploration Rovers (MER) as well as on the Mars Science Laboratory (MSL) rover [1, 2]. While the APXS was calibrated for and intended to determine the chemical composition of solid materials such as rocks and regolith, the MER APXS demonstrated the APXS method was a capable monitor of the atmosphere [3].

Argon (^{40}Ar) comprises approximately 2% of the CO_2-dominated martian atmosphere by volume [4], though local volume mixing ratios (VMR) fluctuate over the course of the martian year (i.e., with Solar Longitude, L_s) [3, 5, 6, 7]. As CO_2 is deposited onto the frost cap, noncondensable gases (NCGs) (e.g., Ar, N_2) concentrate over the winter pole [6]. CO_2 sublimation the following spring creates a global pressure gradient that drives circulation to lower latitudes.

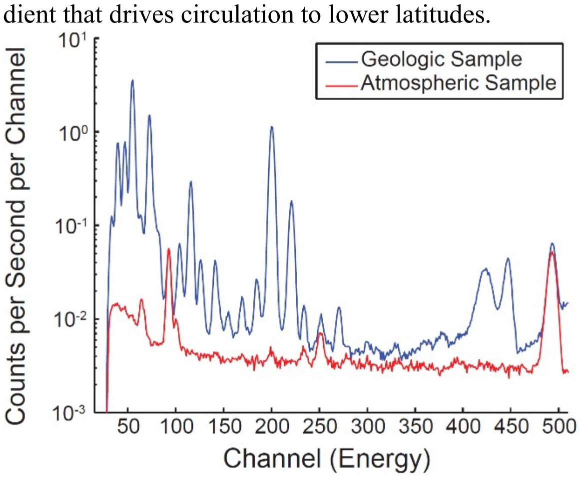

Figure 1: APXS spectra acquired by the MER rover Opportunity. Geologic spectrum (blue) corresponds to a measurement duration of 11.5 hours. Atmospheric spectrum (red) corresponds to a measurement duration of 16 hours. The argon peak is visible around channel 100, where the atmospheric spectrum overlaps the geologic spectrum. Figure from [3].

Ar provides the only characteristic X-rays detected by the APXS that are sourced from the atmosphere – the remaining peaks are from the instrument itself. **Figure 1** offers a comparison of geologic (blue) and atmospheric (red) spectra acquired by the MER generation APXS. The Ar peak is visible around channel 100. The majority of the Ar signal originates from the column of air inside the MER APXS instrument [3, 8]. The MSL APXS instrument has a more compact design and thus can acquire spectra at closer proximity to the target surface. As a result, Ar peaks in MSL APXS geologic spectra present as a shoulder between the characteristic Cl and K peaks, when placed in contact with the surface.

Separated by thousands of kilometers in the equatorial region of Mars, the MER and MSL APXS instruments have operated as three high-frequency atmospheric monitoring stations over the course of several Mars years (MY), capable of tracking the flow of NCGs using Ar as a tracer. Collectively the instruments have acquired thousands of hours of atmospheric spectra. These data provide ground-based observations for global climate models (e.g., [5]) and complement high-precision measurements of NCGs (e.g., such as those by MSL SAM [7]) and those of the bulk atmosphere (e.g., MSL REMS [9]).

Method: APXS atmospheric spectra are analyzed following the method of [3]. Ar peak areas are calculated using a channel-sum model, subtracting the appropriate background as dictated by channels adjacent to those of the peak. The resulting Ar peak areas are corrected for temperature and source activity. In the process, the APXS is able to trace condensation flow at low-latitudes through relative changes in Ar peak area within atmospheric spectra (e.g., **Figure 2**).

Following the work of [3], dedicated, and often parallel, measurements with the MER-B and MSL APXS instruments were conducted during the MY 34 L_s 150 timeframe to monitor the previously observed short-term spike in NCGs (Ar). Simultaneous measurements between the MSL APXS and SAM were also acquired (**Figure 3**).

Currently (Q1 2020), MSL is experiencing the MY 35 transition to southern spring and summer. An increased APXS atmospheric measurement cadence is underway once again to monitor the change in Ar partial pressure (p_{Ar}) at Gale Crater. Results through to approximately MY 35 L_s 160 will be presented at the conference, encompassing the MY 35 L_s 150 timeframe.

Results: MSL APXS atmospheric measurements are consistent with those previously acquired by its

MER predecessor. MER-B quality atmospheric measurement durations exceed the MSL total by a factor of ~6x. All APXS p_{Ar} data are currently not corrected for changes in elevation; this is anticipated to be a minor effect.

Figure 2 captures MSL p_{Ar} results as a function of MY. Reduced MER-B data are underlain for comparison, as is a periodic sinusoidal fit of the MER data. A polynomial curve representative of the total pressure observed by REMS (from [7]) is also illustrated.

The MSL data plotted in **Figure 2** have not been reduced and thus present as noisier data compared to MER. A short-term spike in p_{Ar} appears to be present in the MSL MY 34 APXS data, coinciding with approximately the same timeframe as was observed by MER-B [3].

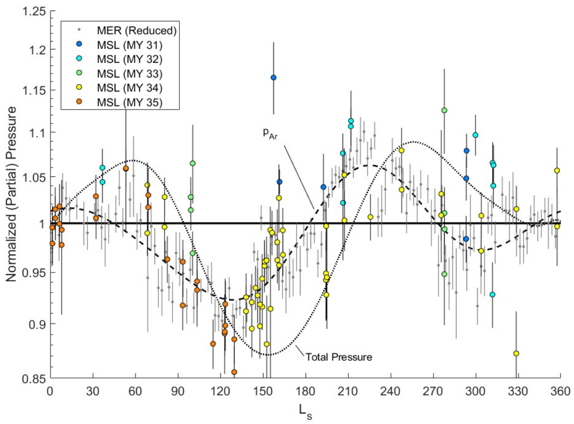

Figure 2: MER-B and MSL APXS Ar partial pressure (p_{Ar}), normalized to L_s 0. MER data are reduced (i.e., statistics improved through spectral reduction). Dashed line is a periodic fit of the reduced MER-B APXS p_{Ar} data, excluding regions of short-term enrichment (e.g., L_s 150). The dotted line represents typical atmospheric pressure variation. The phase shift whereby p_{Ar} leads p_{Tot} ($\approx p_{CO2}$) by ~30° L_s is a result of condensation flow, as observed at low latitudes.

The p_{Ar} data in **Figure 2** can be expressed as a mixing ratio (MR) to support direct comparison with MSL SAM data (from [7]). Ar MR is derived through the ratio of p_{Ar} to p_{Tot}. That is, Ar MR is estimated from the APXS-derived p_{Ar} divided by the pressure observed by REMS. This was conducted for both MER-B and MSL data sets. Normalization largely corrects for the utilization of data at different landing sites and from different instruments.

APXS Ar MR data from both MER-B and MSL are plotted in **Figure 3**. VMR data from MSL SAM is overlaid for direct comparison. Both data sets are in excellent agreement. While the APXS is not able to quantitatively measure the absolute partial pressure of Ar in the atmosphere, its high-frequency capabilities do complement the high-accuracy but low-frequency measurements by SAM.

Ground data and modern global climate models (MarsMPAS, [5]) are also in good agreement. As first captured in MER APXS data [3], MarsMPAS also predicts the presence of a double-peak feature in NCGs near autumn equinox, though ~25 L_s earlier. The timing difference between the observed and simulated temporal argon mixing ratio may result from inadequate numerical representation of argon transport due to interactions among thermally direct/indirect circulations, condensation flow associated with CO_2 cycle, and eddy mixing. Thus, the ground-based rover data may help improve our understanding of transport phenomena at low latitudes since the enrichment and dilution of NCGs, resulting from CO_2 condensation and sublimation, is limited to high (≥50°) latitudes.

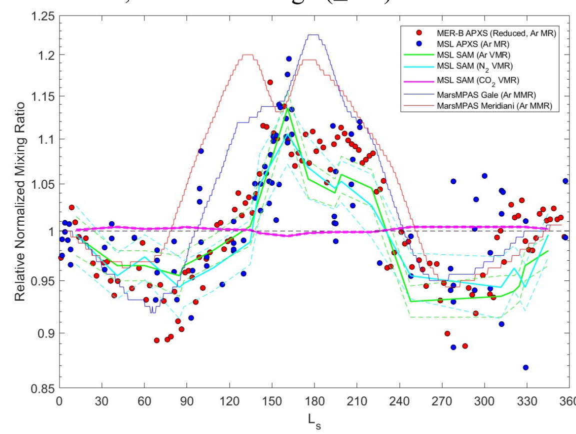

Figure 3: MER-B and MSL APXS Ar MR normalized to L_s 0. Data from MSL SAM (Ar, N_2, and CO_2 VMRs, from [7]) are normalized and overlaid for direct comparison. APXS error bars are not plotted but are comparable to **Figure 2**; SAM errors are represented by dashed lines. MarsMPAS [5] Ar mass-mixing ratio (MMR) for Gale (blue) and Meridiani (red) are included. Ar MMR ≈ Ar VMR as CO_2 and Ar are of similar molecular mass. SAM and APXS data were acquired over multiple MYs (e.g., **Figure 2**).

Acknowledgments: This work was supported by NASA/Caltech/JPL and by the Canadian Space Agency. Much appreciation goes to NASA/JPL for their support, dedication, and invaluable expertise during development and operations of both the MER and MSL missions. The development of MarsMPAS was supported by NASA grant 80NSSC18K0089.

References:

[1] Gellert et al., (2006), JGR, 111.
[2] Gellert et al., (2015), Elements, 11.
[3] VanBommel et al., (2018), JGR, 123.
[4] Franz et al., (2017), PSS, 138.
[5] Lian et al., (2018), AGU, P33B-07.
[6] Sprague et al., (2012), JGR, 117.
[7] Trainer et al., (2019), JGR, 124.
[8] VanBommel et al., (2019), NIM:B, 441.
[9] Martínez et al., (2017), SSR, 212.